11th International Symposium on Magnetic Bearings
August 26-29, Nara, Japan

DECOUPLED CONTROL USING REDUNDANT COORDINATES FOR THREE-POLE HYBRID ACTIVE MAGNETIC BEARING SYSTEM

Sang-Hyun Park
Center for Noise and Vibration Control, KAIST Science Town, Daejeon 305-701, Korea
ppark-0525@kaist.ac.kr

Chong-Won Lee
Center for Noise and Vibration Control, KAIST Science Town, Daejeon 305-701, Korea
cwlee@ kaist.ac.kr

ABSTRACT
In this paper, we propose a bearing redundant coordinates and decoupled PD controller for 5-axis active magnetic bearing system, which consists of two bearing parts such as three-pole hybrid active magnetic bearing to stabilize the radial direction and ring-type permanent magnetic bearing stabilizing in axial and tilting motion. Based on derived system equation with decoupled control scheme, we examine controllability and observability as well as numerical modal analysis. The experiments are also carried out in order to verify the effectiveness of the proposed controller in stabilizing the transient and steady state response of the rotor.

INTRODUCTION
In recent years, design of low-cost miniaturized active magnetic bearings (AMBs) becomes increasingly important, as they find potential applications to hard disk drive [1], artificial heart blood pump [2,3], etc. There have been many attempts for more compact and cost-effective design ideas for such AMBs. Idea of three-pole permanent magnet biased AMB has been proposed not only to provide the compactness of design but to reduce the number of power amplifiers as well as the power consumption. But, it suffers from the nonlinear, coupled and asymmetric behaviors with current and stiffness coefficient matrices, which is not desirable for controller design.
To make the AMB as compact as possible, it is needed to reduce the number of actuators. In this paper, we employ the axially polarized ring type permanent magnet bearings to stabilize the axial and tilting motion of the vertical rotor. Another important design improvement is to intentionally introduce the pole-shoe in order to utilize the Hall diodes with high sensitivity. This may reduce the cost of sensor part in AMBs.
Three-pole electro-magnet configuration, compared with the conventional four- or eight-pole electro-magnetic configuration, inherently introduces a control redundancy because three independent electro-magnetic actuators control the two degrees-of-freedom motion of the rotor. In addition, due to the use of three sub-poles with permanent magnets to generate bias flux, the force-displacement relation becomes highly nonlinear. In this paper, the concept of redundant coordinates is adopted so that the identical controller design for three coordinates can be conveniently achieved. One of the immediate advantages in the use of redundant coordinates is to deal with symmetric system matrices for the linearized control model with respect to the equilibrium position.

CONFIGURATION OF PROPOSED AMBS

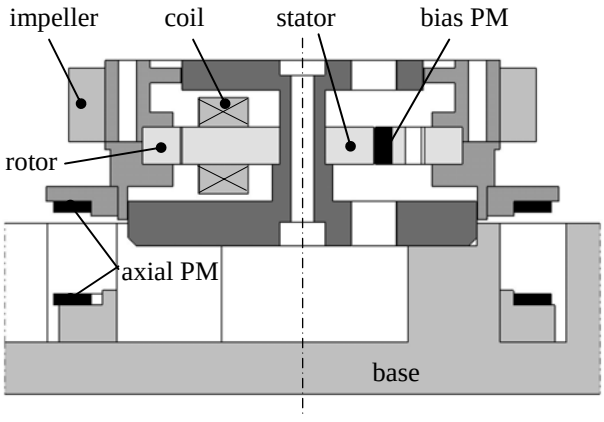

FIGURE 1: Schematic view of the proposed system

Figure 1 shows the schematic view of the proposed system. It consists of radial hybrid-type three-pole active magnetic bearing, which is outer rotor type and axial permanent magnet bearing for 5-axis suspension, which is profitable to more small-sized AMB system. In addition, the proposed system uses the laminated silicon iron for both stator and rotor decrease the eddy current effect. A pair of axially polarized ring type permanent magnets is placed with the same poles facing each other, in order to induce the repulsive force for passive stability in the axial and angular motion.

AXIAL PERMANENT MAGNET BEARING

To make more small-sized AMBs as well as low power consumption, proposed system employs ring type permanent magnet bearing. As the result, the motion of the proposed AMB needs to be controlled only in the radial directions. A pair of axially polarized ring type permanent magnets is place on the stator and rotor, facing each other with opposite poles. This configuration of permanent magnets provides positive stiffness in the axial direction, but negative stiffness in the radial motion whose magnitude is half of the axial stiffness. However, the AMBs can generate the positive radial force large enough to compensate for the resulting unstable radial motion of the rotor. The permanent magnet bearing is designed strong enough to support the weight of the vertical rotor. In axial permanent magnet bearing, three stiffnesses are dominant such as axial stiffness, K_x, radial stiffness, $-K_x/2$, and angular moment stiffness, $R^2K_x/2$. Here R is the radius of permanent magnets.

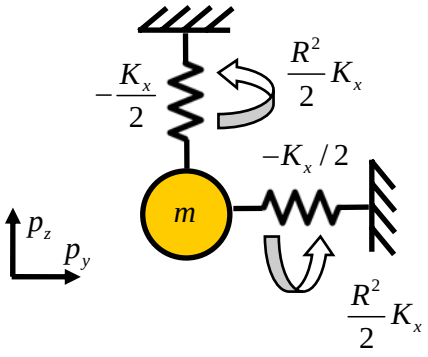

FIGURE 2: Simple model of axial PMB

RADIAL THREE-POLE MAGNET BEARING

The proposed radial three-pole magnetic bearing consists of three main-poles and three sub-poles equally spaced, respectively, along the periphery of the stator by shown Fig. 3(a). This rather unusual configuration makes it hard to construct a linear system model in a usual way. Using the conventional Cartesian coordinates, there appear nonlinear quadratic off-diagonal terms in the stiffness matrix, which cannot be properly expressed by first order linearized stiffness coefficients. This means that the system can only be represented by a non-linear model in the Cartesian coordinates.

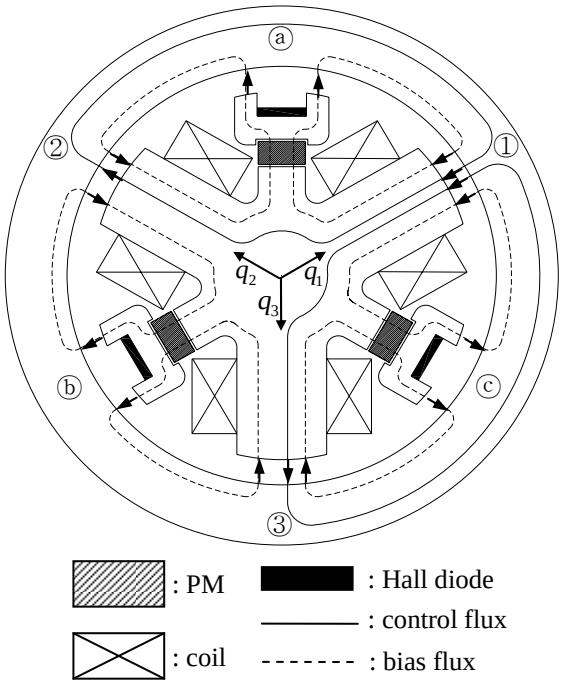

FIGURE 3(a): Magnetic flux path of radial AMB

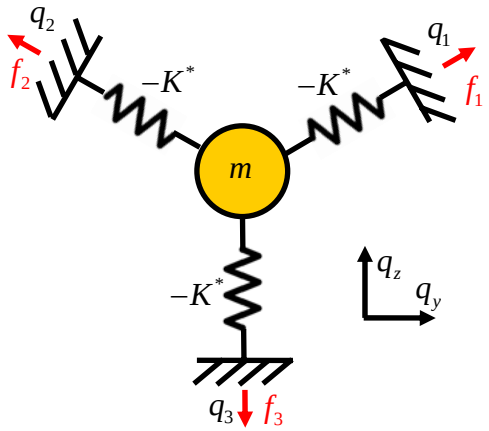

FIGURE 3(b): Simple model of radial AMB

Here, the redundant coordinates are introduced to construct the simple linear model. The proposed redundant coordinates (q_1, q_2, q_3) have the same structure as the configuration of the physical model. Figure 3(b) shows the simple model of the radial three-pole magnetic

bearing part, where K^* and f_k, $k=1\sim3$, are the displacement (negative) stiffness and electromagnetic force at each coordinates. Note that the displacement stiffness of each pole is related with the diagonal and off-diagonal stiffnesses, i.e.

$$K^* = \frac{3}{2}K_{qd} = 3K_{qo} \tag{1}$$
$$K_{qd} \equiv K_{qmn} \ \ (m=n), K_{qo} \equiv K_{qmn} \ \ (m\neq n)$$
$$, K_{qmn} = \frac{\partial F_m}{\partial q_n}, \ (m,n=1,2,3)$$

The current stiffness, K_i is exactly same relation of Eq. (1).

MODELING AND CONTROL OF PROPOSED SYSTEM

The proposed system consists of radial three-pole magnetic bearing and axial permanent magnet bearing. And the control input acts on the radial three-pole magnetic bearing part. For this reason, the bearing redundant coordinates ($q_1, q_2.q_3, p_1, p_2.p_3$) is convenient compared to the C.G. coordinates (y, z, θ_y, θ_z). Here, only two transforms are needed between bearing redundant coordinates and C.G. coordinates given by

$$\mathbf{q^{(6)}} = \mathbf{T_r T_b q_g^{(4)}} \tag{2}$$
$$\mathbf{q_g^{(4)}} = \{y \quad z \quad \theta_y \quad \theta_z\}^T$$
$$\mathbf{q^{(6)}} = \{q_1 \quad q_2 \quad q_3 \quad p_1 \quad p_2 \quad p_3\}^T$$

where $\mathbf{T_r}$ is the transform matrix between physical coordinates (y, z) and redundant coordinates ($1,2,3$) given by [4]

$$\mathbf{q_{yz0}} = \mathbf{T_r q_{123}} \ , where \ \mathbf{q_{yz0}}^{\mathbf{T}} = [y\, z\, 0]^{\mathbf{T}}, \ \mathbf{q_{123}}^{\mathbf{T}} = [1\,2\,3]^{\mathbf{T}}$$
$$\mathbf{T_r} = \frac{2}{3}\begin{pmatrix} \cos\varphi & \cos\left(\varphi-\frac{2\pi}{3}\right) & \cos\left(\varphi+\frac{2\pi}{3}\right) \\ -\sin\varphi & -\sin\left(\varphi-\frac{2\pi}{3}\right) & -\sin\left(\varphi+\frac{2\pi}{3}\right) \\ \frac{1}{2} & \frac{1}{2} & \frac{1}{2} \end{pmatrix} \tag{3}$$

where 0 variable is a dummy variable, which is not associated with the arbitrary reference frame. $\mathbf{T_b}$ is the transform matrix between C.G. coordinates and bearing fixed coordinates.

$$\mathbf{q^{(4)}} = \mathbf{T_b q_g^{(4)}} \tag{4}$$

$$\mathbf{T_b} = \begin{bmatrix} 1 & 0 & 0 & b_a \\ 0 & 1 & -b_a & 0 \\ 1 & 0 & 0 & -b_p \\ 0 & 1 & b_p & 0 \end{bmatrix}, \mathbf{q^{(4)}} = \begin{Bmatrix} y_a \\ z_a \\ y_p \\ z_p \end{Bmatrix}, \mathbf{q_g^{(4)}} = \begin{Bmatrix} y \\ z \\ \theta_y \\ \theta_z \end{Bmatrix}$$

here, sub-script a and p mean that the radial magnetic bearing and permanent magnetic bearing. b_a and b_p are the distances of two bearings from the C.G. point of the rotor.

To derive the equation of motion, the Lagrangian, L for conservative system is needed with respect to C.G. given by

$$L = T - V$$
$$T = \frac{1}{2}m\left\{\dot{y}^2 + \dot{z}^2\right\} + \frac{1}{2}J_d\left\{\dot{\theta}_y^{\,2} + \dot{\theta}_z^{\,2}\right\} - J_p\theta_y\dot{\theta}_x\dot{\theta}_z$$
$$V = \frac{1}{2}\left(-K^*\right)\left\{\dot{q}_1^{\,2} + \dot{q}_2^{\,2} + \dot{q}_3^{\,2}\right\} + \frac{1}{2}\left(-\frac{K_x}{2}\right)\left\{\dot{y}_p^{\,2} + \dot{z}_p^{\,2}\right\} \tag{5}$$
$$+ \frac{R^2}{4}\left(K_x\right)\left\{\theta_y^{\,2} + \theta_z^{\,2}\right\}, \ where, \dot{\theta}_x = \Omega$$

here, m is the mass of the rotor, R is the radius of the permanent magnet bearing, J_p and J_d are the polar moment of inertia and diametrical moment of inertia at each, K^* and K_x are displacement stiffness of radial magnetic bearing and axial stiffness of axial PM bearing, and Ω is the rotational speed of the rotor. Note that the gyroscopic moment and moment force due to the permanent magnetic bearing, which is significant on disk-type rotor. Using the Lagrangian, L, the Lagrange equation of motion is needed for deriving the system equation. Here, the system model is four degree of freedom excluding axial direction, x, where as coordinates' variables are six ($q_1, q_2.q_3, p_1, p_2.p_3$), which means that there are needed two holonomic constraints exist given by

$$g_1 : q_1 + q_2 + q_3 = 0$$
$$g_2 : p_1 + p_2 + p_3 = 0 \tag{6}$$

This means that Lagrangian equation of motion for holonomic constraints is needed given by [5]

$$\frac{d}{dt}\left(\frac{\partial L}{\partial \dot{q}_k}\right) - \frac{\partial L}{\partial q_k} = \sum_{l=1}^{m}\lambda_l a_{lk}$$
$$q_k = q_1, q_2, q_3, p_1, p_2, p_3 \quad m = 2, \ a_{lk} = \frac{\partial g_l}{\partial q_k} \tag{7}$$

here, L is the Lagrangian defined for a conservative system, and λ_l is the Lagrange multiplier, which is a required force to satisfy the constraint condition in Eq.

(6). The equation of motion in Eq. (5) may be rewritten about the bearing redundant coordinate using transform matrix in Eqs. (3) and (4) considering the constraint condition given by

$$\boldsymbol{M}\ddot{\boldsymbol{x}} + \boldsymbol{G}\dot{\boldsymbol{x}} + \boldsymbol{K}\boldsymbol{x} = \boldsymbol{f}$$
$$, \boldsymbol{x} = \{q_1 \quad q_2 \quad q_3 \quad p_1 \quad p_2 \quad p_3\}^T \tag{8}$$

here $\boldsymbol{M}$, $\boldsymbol{G}$, $\boldsymbol{K}$, $\boldsymbol{f}$ are inertia, gyroscopic, stiffness, and electro magnetic force. Note that $\boldsymbol{M}$ and $\boldsymbol{K}$ are mutually coupled between active and permanent magnet bearings, and confirmed that the skew symmetric property in $\boldsymbol{G}$ [A.1]. And Lagrange multipliers can be obtained like as

$$\lambda_q = -\frac{1}{3}\{f_1 + f_2 + f_3\}, \lambda_p = 0 \tag{9}$$

The magnetic force, $\boldsymbol{f}$ can be expressed in substituting Eq. (9) into (8).

$$\boldsymbol{f} = \frac{1}{3}\begin{bmatrix} 2 & -1 & -1 \\ -1 & 2 & -1 \\ -1 & -1 & 2 \\ 0 & 0 & 0 \\ 0 & 0 & 0 \\ 0 & 0 & 0 \end{bmatrix}\begin{Bmatrix} f_1 \\ f_2 \\ f_3 \end{Bmatrix} \tag{10}$$

Here, it is confirmed that electro magnetic force acts on radial magnetic bearing part with mutually coupled.
To stabilize the system, the identical PD controller is employed at each electro magnet given by

$$f_j = K_i i_j = -K_i K_A K_s \left[K_P q_j + K_d \dot{q}_j\right], \; j = 1,2,3 \tag{11}$$

where K_i is a current stiffness and i_j is the control current at each pole. K_s K_A are sensor and power amplifier gain at each. K_P and K_d are the P- and D-gains, respectively, of the controller. When decoupled PD controller in Eq. (11) is employed, magnetic force, $\boldsymbol{f}$, in Eq. (10) can be rewritten by

$$\boldsymbol{f} = \boldsymbol{K}_p^* \begin{Bmatrix} q_1 \\ q_2 \\ q_3 \end{Bmatrix} + \boldsymbol{K}_d^* \begin{Bmatrix} \dot{q}_1 \\ \dot{q}_2 \\ \dot{q}_3 \end{Bmatrix} \tag{12}$$
$$, \boldsymbol{K}_p^* = \begin{bmatrix} diag\left[K_p^*\right]_{3\times3} \\ [\boldsymbol{0}]_{3\times3} \end{bmatrix}, \boldsymbol{K}_d^* = \begin{bmatrix} diag\left[K_d^*\right]_{3\times3} \\ [\boldsymbol{0}]_{3\times3} \end{bmatrix}$$

Here, the electro magnetic force can be decoupled. This means that applying the identical PD control scheme, the system equation can be diagonalized and system equation in Eq. (8) may be expressed by

$$\boldsymbol{M}\ddot{\boldsymbol{x}} + (\boldsymbol{G} + \boldsymbol{K}_d^*)\dot{\boldsymbol{x}} + (\boldsymbol{K} + \boldsymbol{K}_p^*)\boldsymbol{x} = \boldsymbol{0} \tag{13}$$

Note that the electro magnetic force affect the whole system such as active and permanent magnet bearing, because system is mutually coupled.

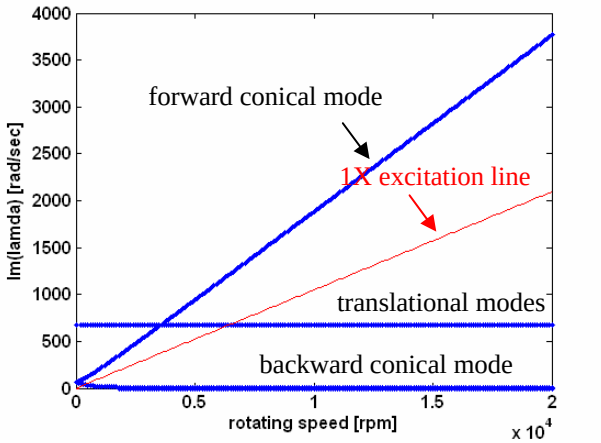

FIGURE 4(a): Whirl speed chart for proposed system

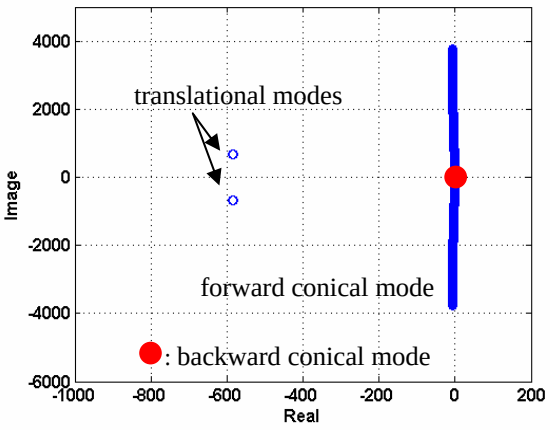

FIGURE 4(b): Root-locus increasing rotating speed

Figure 4(a) and 4(b) show the whirl speed chart and root locus plot at each. It is confirmed that the disk type rotor which is dominant on the gyroscopic effect shown Fig. 4(a). In root locus plot, Fig. 4(b), backward and forward conical modes have almost small damping due to the passive stability using axial permanent magnet bearing while translational modes have sufficient damping.

MODAL CONTROLLABILITY/OBSERVABILITY

For examining the modal controllability and observability of proposed system using decoupled PD controller, Eq.

(13) is described in the state space representation as follows:

$$\dot{X} = AX + Bu$$
$$Y = CX,\ X^T = \begin{bmatrix} q_i & p_i & \dot{q}_i & \dot{p}_i \end{bmatrix}^T \quad (14)$$

where

$$A = \begin{bmatrix} 0 & I \\ -M^{-1}(K + K_p^*) & -M^{-1}(G + K_d^*) \end{bmatrix},$$
$$B = \begin{bmatrix} 0 & 0 \\ -M^{-1}K_p^* & -M^{-1}K_d^* \end{bmatrix}, C = \begin{bmatrix} I & 0 & I & 0 \end{bmatrix}$$

Here, we can describe the above system by using modal decomposition $\Phi\Lambda\Psi^T$ as

$$\dot{X} = \Phi\Lambda\Psi^T X + Bu \quad (15)$$

where $\Lambda \in R^{12\times12}$ is the diagonal matrix of eigenvalues, and $\Phi \in R^{12\times12}$ and $\Psi \in R^{12\times12}$ are the right and the left modal matrices whose columns consist of the right and the left eigenvectors of the system matrix, A. If the initial value is assumed to be zero, then the output response of the system in Eq. (15) can be obtained as

$$Y = C\Phi\int_0^{t_f} e^{\Lambda(t-\tau)}\{\Psi^T B\}u(\tau)d\tau, \qquad Y(0) = 0 \quad (16)$$

In Eq. (16), the matrix term $\Psi^T B$ represents the channel from control input to system's modes and the matrix $C\Phi$ represents the channel from system's modes to output. These two matrices are closely related with system's controllability and observability. Based on that, the modal controllability and observability can be given by [6]

$$\text{Modal controllability, } \nu_{ij} = \cos\theta_{ij} = \frac{|\psi_i^T \cdot b_j|}{\|\psi_i\|\|b_j\|} \quad (17)$$

$$\text{Modal observability, } \mu_{ki} = \cos\delta_{ki} = \frac{|c_k \cdot \phi_i|}{\|c_k\|\|\phi_i\|} \quad (18)$$

Here, ν_{ij} reflects the degree of controllability of i th mode from j th control input. μ_{ki} is taken to be an indication for the degree of observability of the i th mode to k th output. Figures 5(a) and 5(b) shows the modal controllability and observability of proposed system increasing rotational speed.

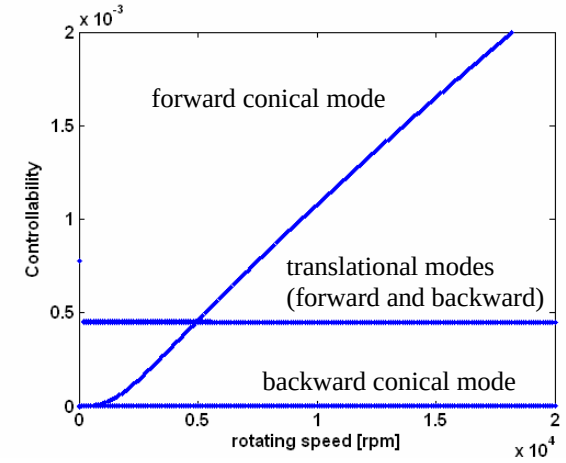

FIGURE 5(a): Modal controllability of proposed system

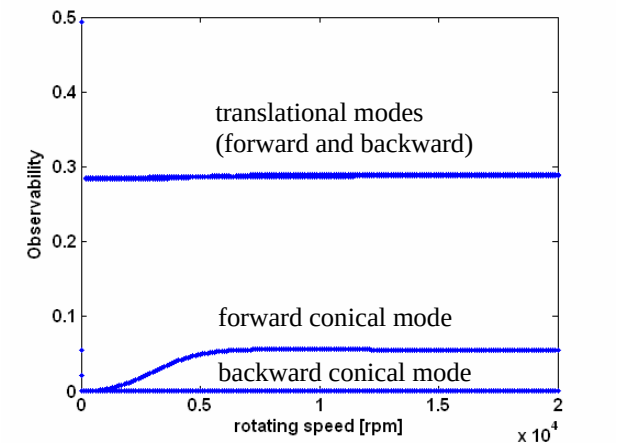

FIGURE 5(b): Modal observability of proposed system

Above these figures, they show that the low controllability and observability in backward conical mode due to the axial permanent magnet bearing with low damping.

EXPERIMENTAL RESULTS

Figure 6 shows the experimental setup to test the performance of the prototype AMB system developed in the laboratory. During the tests, two compressed air nozzles of maximum pressure equal to 3×10^5 Pa were placed opposite to each other to exert a pure torque to the rotor. The specifications of the proto type are listed in table 1.

The levitation test of the prototype AMBs has been performed at rest from its dead weight equilibrium with identical PD controller (P-gain: 3.0, D-gain: 0.003). Figure 7(a) shows the typical transient response of the rotor when the levitation control action starts at 2.04 second. Note that the rotor position is quickly stabilized within about 0.1 second and the residual displacement

remained less than 10㎛ mainly due to axial and tilting modes about 10*Hz*. The maximum control current to each power amplifier was less than 1.0 *A* and the steady-state residual current was kept below 10 *mA*, which is quite satisfactory. Not that since the axial and tilting motions are passively stable, they have very low damping which may affect the system stability.

TABLE 1: Design parameters

Stator		Rotor	
Diameter	32 mm	Outer diameter	42.4 mm
Thickness	10 mm	Inner diameter	32.4 mm
Thickness of PM	2 mm	Air gap	0.2 mm
No. of PM	3	Rotor mass	166 g
No. of Coil	75		

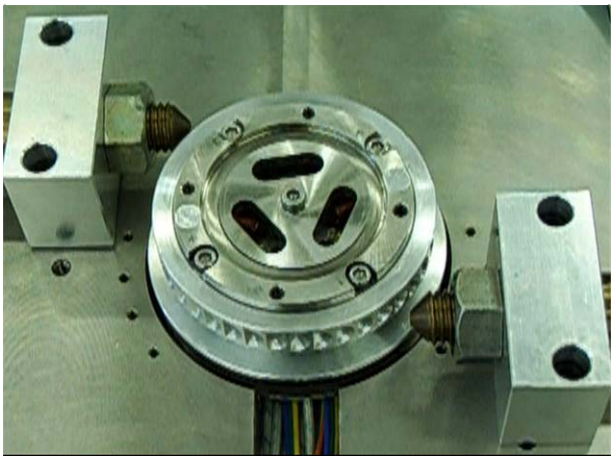

FIGURE 6: Experimental setup of proposed AMBs

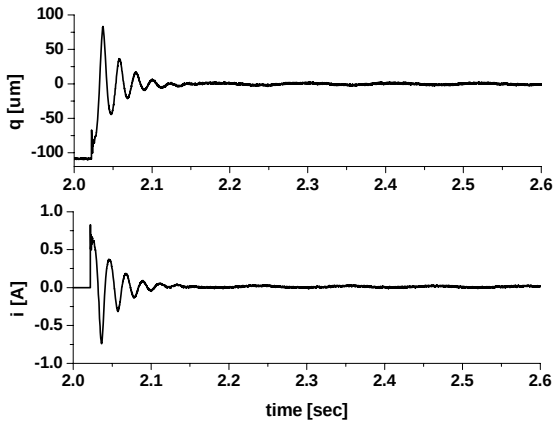

FIGURE 7(a): Transient response

In a speed-up test, the rotor could successfully rotate over 5,000 rpm as it was levitated. Figure 7(b) shows the radial vibration at every 200 rpm. There was large amplitude at 800 rpm due to the axial mode with low damping, and vibration was well suppressed under 30㎛. Considering the nominal air gap of 200㎛ (the clearance of touch-down bearing is 120㎛), the rotor could be driven to a rotating speed up to 5000 rpm without touching any of the surrounding components.

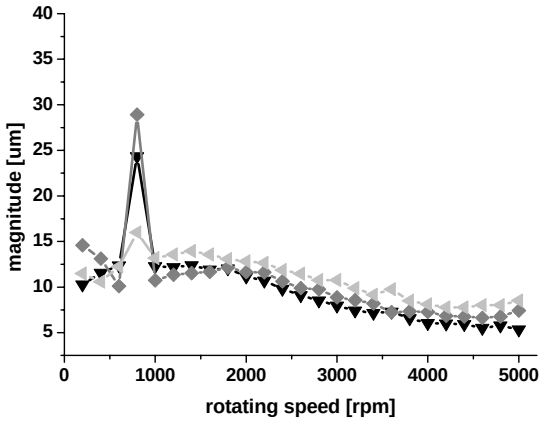

FIGURE 7(b): Radial vibration increasing rotational speed

CONCLUSIONS

We propose the redundant coordinates and identical PD control scheme. These are employed for linear modeling and controller design of the three-pole AMB, which has an inherent nonlinearity, when formulated in the conventional Cartesian coordinates, due to its configuration. Based on redundant coordinates and its equation of motion, modal analysis and modes' controllability are numerically examined. To verify the proposed control scheme, a prototype AMB was built for its performance test, where only the radial motions were actively controlled, while the tilting and axial motions were passively stabilized by the permanent magnets. The proposed AMB succeeded in achieving the stable levitation and rotation up to 5000 rpm.

APPENDIX A.

The equation of motion using bearing redundant coordinates is given by

$$\boldsymbol{M}\ddot{\boldsymbol{x}}+\boldsymbol{G}\dot{\boldsymbol{x}}+\boldsymbol{K}\boldsymbol{x}=\boldsymbol{f} \qquad ,where\ \boldsymbol{x}=\{q_1 \quad q_2 \quad q_3 \quad p_1 \quad p_2 \quad p_3\}^T$$

Here $\boldsymbol{M}$, $\boldsymbol{G}$, $\boldsymbol{K}$, $\boldsymbol{f}$ are inertia, gyroscopic, stiffness, and electro magnetic force expressed by

$$\boldsymbol{M}=\frac{2}{3}\begin{bmatrix} \left(j_d+ml_p{}^2\right) & 0 & 0 & \left(-j_d+ml_al_p\right) & 0 & 0 \\ 0 & \left(j_d+ml_p{}^2\right) & 0 & 0 & \left(-j_d+ml_al_p\right) & 0 \\ 0 & 0 & \left(j_d+ml_p{}^2\right) & 0 & 0 & \left(-j_d+ml_al_p\right) \\ \left(-j_d+ml_al_p\right) & 0 & 0 & \left(j_d+ml_a{}^2\right) & 0 & 0 \\ 0 & \left(-j_d+ml_al_p\right) & 0 & 0 & \left(j_d+ml_a{}^2\right) & 0 \\ 0 & 0 & \left(-j_d+ml_al_p\right) & 0 & 0 & \left(j_d+ml_a{}^2\right) \end{bmatrix}$$

$$\boldsymbol{G}=\frac{2\sqrt{3}j_p\Omega}{9}\begin{bmatrix} 0 & 1 & -1 & 0 & -1 & 1 \\ -1 & 0 & 1 & 1 & 0 & -1 \\ 1 & -1 & 0 & -1 & 1 & 0 \\ 0 & -1 & 1 & 0 & 1 & -1 \\ 1 & 0 & -1 & -1 & 0 & 1 \\ -1 & 1 & 0 & 1 & -1 & 0 \end{bmatrix} \tag{A.1}$$

$$\boldsymbol{K}=\begin{bmatrix} \left(\frac{2R^2}{3b_t{}^2}\frac{K_x}{2}-K_r{}^*\right) & 0 & 0 & -\frac{2R^2}{3b_t{}^2}\frac{K_x}{2} & 0 & 0 \\ 0 & \left(\frac{2R^2}{3b_t{}^2}\frac{K_x}{2}-K_r{}^*\right) & 0 & 0 & -\frac{2R^2}{3b_t{}^2}\frac{K_x}{2} & 0 \\ 0 & 0 & \left(\frac{2R^2}{3b_t{}^2}\frac{K_x}{2}-K_r{}^*\right) & 0 & 0 & -\frac{2R^2}{3b_t{}^2}\frac{K_x}{2} \\ -\frac{2R^2}{3b_t{}^2}\frac{K_x}{2} & 0 & 0 & \left(\frac{2R^2}{3b_t{}^2}-\frac{2}{3}\right)\frac{K_x}{2} & 0 & 0 \\ 0 & -\frac{2R^2}{3b_t{}^2}\frac{K_x}{2} & 0 & 0 & \left(\frac{2R^2}{3b_t{}^2}-\frac{2}{3}\right)\frac{K_x}{2} & 0 \\ 0 & 0 & -\frac{2R^2}{3b_t{}^2}\frac{K_x}{2} & 0 & 0 & \left(\frac{2R^2}{3b_t{}^2}-\frac{2}{3}\right)\frac{K_x}{2} \end{bmatrix}$$

$$\boldsymbol{f}=\left\{f_1+\lambda_q \quad f_2+\lambda_q \quad f_3+\lambda_q \quad \lambda_p \quad \lambda_p \quad \lambda_p\right\}^T$$

, where

$$j_d=J_d/b_t{}^2, j_p=J_p/b_t{}^2, l_a=b_a/b_t, l_p=b_p/b_t, b_t=b_a+b_p$$

REFERENCES

1. Vuillemin, R., Aeschlimann, B., etc., Low cost active magnetic bearings for Hard Disk Drive spindle motors, Proc. of the 6th Int. Symp. on Magnetic Bearings, MIT Cambridge, USA, pp. 3-9, Honor Paper, 1998.

2. Masuzawa, T., Kojima, J., Onuma, H., Okada, Y., Nishida, M., and Yamane, T., Micro magnetic bearing for an axial flow artificial heart, Proc. of the 9th Int. Symp. on Magnetic Bearings, Lexington, Kentucky, USA, August 3-6, 2004.

3. Onuma, H., Murakami, M., and Masuzawa, T., Design of the permanent magnet bearing of the maglev artificial heart, Proc. of the 9th Int. Symp. on Magnetic Bearings, Lexington, Kentucky, USA, August 3-6, 2004.

4. Krause, P. C., *Analysis of Electric Machinery*, McGraw-Hill Book Company, PA, 1986.

5. Meirovitch, L., *Methods of Analytical Dynamics*, McGraw-Hill Book Company, 1970.

6. Hamdan, A. M. A. and Nayfeh, A. H., Measures of modal controllability and observability for first- and second-order linear system, Journal of Guidance, control, and Dynamics, Vol. 12, No. 3. pp. 421-428., 1989.

7. Reisinger, M., Amrhein, W., and Silber, S., Development of a Low Cost Permanent Magnet Biased Bearing, Proc. of the 9th Int. Symp. on Magnetic Bearings, Lexington, Kentucky, USA, August 3-6, 2004.

8. Okada, Y., Koyanagi, H., Kakihara, K., and Ueno, S., MiracBearing New Concept of Miracle Magnetic Bearings, Proc. of the 9th Int. Symp. on Magnetic Bearings, Lexington, Kentucky, USA, August 3-6, 2004.

9. Hsu, C. T., and Chen, S. L., Nonlinear control of a 3-pole active magnetic bearing system, Journal of Automatica, Vol. 39, No.2, pp. 291-298, 2003.

10. Schweitzer, G., Active magnetic bearings-chances and limitations, Proc. of the 6th IFToMM Int. Conf. on Rotor Dynamics, Sydney, pp1-14, 2002.

11. Lee, C. W., Mechatronics in rotating machinery, Proc. of the 8th IFToMM Int. Conf. on Rotor Dynamics, Vienna, keynote paper, 2006.